A Simple Molecular Model for Thermophilic Adaptation of Functional Nucleic Acids†

Joshua M. Blose,‡ Scott K. Silverman,§ and Philip C. Bevilacqua*,‡

Department of Chemistry, The Pennsylvania State University, University Park, Pennsylvania 16802, and Department of Chemistry, University of Illinois at Urbana-Champaign, 600 South Mathews Avenue, Urbana, Illinois 61801

Received September 26, 2006; Revised Manuscript Received January 8, 2007

ABSTRACT: RNA molecules have numerous functions including catalysis and small molecule recognition, which typically arise from a tertiary structure. There is increasing interest in mechanisms for the thermostability of functional RNA molecules. Sosnick, Pan, and co-workers introduced the notion of "functional stability" as the free energy of the tertiary (functional) state relative to the next most stable (nonfunctional) state. We investigated the extent to which secondary structure stability influences the functional stability of nucleic acids. Intramolecularly folding DNA triplexes containing alternating T•AT and C^+•GC base triples were used as a three-state model for the folding of nucleic acids with functional tertiary structures. A four-base-pair tunable region was included adjacent to the triplex-forming portion of the helix to allow secondary structure strength to be modulated. The degree of folding cooperativity was controlled by pH, with high cooperativity maintained by lower pH (5.5), and no cooperativity by higher pH (7.0). We find a linear relationship between functional free energy and the free energy of the secondary structure element adjacent to tertiary interactions, but only when folding is cooperative. We translate the definition of functional stability into equations and perform simulations of the thermodynamic data, which lend support to this model. The ability to increase the melting temperature of tertiary structure by strengthening base-pairing interactions separate from tertiary interactions provides a simple means for evolving thermostability in functional RNAs.

RNA can perform many functions in the cell such as chemical catalysis, small molecule binding, and protein binding (*1*−*6*). Functional RNAs include ribozymes, riboswitches, and ribosomal and transfer RNAs. This diversity of RNA function has led to increased interest in the pathways by which RNA folds into the native state (*7*−*11*). In general, the native state of a functional RNA has a tertiary structure that rivals those of proteins in terms of molecular complexity (*12*). In comparison, the secondary structures of nucleic acids are rather simple, and their stabilities are dominated by the molecular recognition principles of Watson−Crick base pairing (*13*).

One of the features that distinguishes the RNA and protein folding problems is the unusually high stability of secondary structure in RNA. Indeed, the basic secondary structural elements of RNA, such as duplexes, hairpins, and internal loops, can be studied in model oligonucleotides that are fully stable in the absence of additional secondary or tertiary structural elements (*13*). Tertiary folding typically involves the association of preformed secondary structural elements, making the kinetics and thermodynamics of RNA folding largely hierarchical (*14*, *15*). The experiments herein explore the thermodynamics of hierarchical folding.

Hierarchical folding of RNA opens the possibility for thermodynamic coupling between various folding steps. Coupling between secondary and tertiary structure folding has been clearly established for several RNAs. Early work from Crothers and co-workers showed that, in the presence of low concentrations of Mg^{2+}, tRNA unfolds through a number of detectable intermediates (*16*). Stein and Crothers later demonstrated that, in the presence of higher concentrations of Mg^{2+}, tRNA unfolds in an apparent two-state fashion in which the tertiary structure is more stable than certain secondary structural elements (*17*). Mg^{2+}-dependent coupling of secondary and tertiary structure folding has been shown in other RNAs including the 58 nt L11-binding domain from 23S rRNA (*18*), a pseudoknot from the *Escherichia coli* α mRNA leader (*19*), and a pseudoknot from the T2 bacteriophage autoregulatory mRNA leader (*20*).

There has been intense interest in the mechanisms by which proteins achieve thermostability, reviewed in (*21*). Among the mechanisms suggested are strengthening of tertiary interactions through van der Waals contacts, hydrogen bonding, and the hydrophobic effect. In addition, decreasing the size of loops and strengthening of secondary structure have been identified as contributing to protein thermostability. Comparatively less is understood about how functional RNAs achieve thermostability.

Sequence comparison suggests that the strength of secondary structural interactions plays an important role in the thermostability of functional RNA. For example, despite no correlation of *genomic* GC-content with optimal growth

† This work was supported by NSF Grant MCB-0527102 to P.C.B.

* Author to whom correspondence should be addressed. Tel: (814) 863-3812. Fax: (814) 863-8403. E-mail: pcb@chem.psu.edu.

‡ The Pennsylvania State University.

§ University of Illinois at Urbana-Champaign.

10.1021/bi0620003 CCC: $37.00 © 2007 American Chemical Society
Published on Web 03/16/2007

temperature of the organism, thermophilic rRNAs, tRNAs, and RNase P RNAs have much greater GC-content and fewer secondary structure defects than their mesophilic counterparts (*22*−*24*); moreover, there is a correlation between predicted melting temperatures of the secondary structure of RNA molecules and the optimal growth temperature of the organism in which they are found (*25*). In addition, *in vitro* evolution experiments for RNAs with thermostable tertiary structure have revealed conversion of GU wobble pairs to Watson−Crick AU and (mostly) GC pairs (*26*). Other factors such as strengthening of tertiary interactions, macromolecular crowding, and protein interactions likely contribute to the temperature stability of thermophilic RNAs as well. Nonetheless, the striking correlation between secondary structure stability and thermophilicity suggests that secondary structure stability plays a major role in the thermostability of functional RNA. Despite these observations, a quantitative molecular model has not been advanced for how secondary structure stability affects thermostability of functional nucleic acids.

Sosnick, Pan, and co-workers introduced the concept of "functional stability", which is defined from the viewpoint of biological function (*8*). To have function, native tertiary structure is necessary; as such, functional stability is defined as the free energy difference between the native state and the penultimately stable nonfunctional state, whatever its identity. This definition leaves open the intriguing possibility that in a non-two-state system the identity of the penultimately stable state (i.e., reference state) can change with temperature.

In the present study, we relate the concept of functional stability to thermostability by deriving equations that relate the empirically measurable concentrations of the various folded states to temperature. We also relate functional stability to the temperature at which tertiary structure melts, or the tertiary melting temperature (TMT[1]). We examine whether coupling of secondary and tertiary folding steps provides a plausible model for how strengthening base pairing can affect functional stability. Although earlier studies were pioneering in establishing coupling in the hierarchical folding of RNA, they were limited in their ability to establish a quantitative relationship between secondary structure stability and thermostability. One limitation was that the RNAs studied have very complex folding pathways involving four (*20*, *27*), five (*16*), or seven (*19*) discrete states; moreover, the unfolding pathways involved one or more branched steps. In addition, the secondary structural elements probed by AU-for-GC base pairing swaps (*18*−*20*, *28*−*30*) were often embedded in the tertiary elements themselves, which leaves open the possibility that the base pairing swaps affected the stability of tertiary interactions directly, rather than indirectly. Because of these complications, the authors typically interpreted the effects of base pair swaps qualitatively, using them to assign various folding transitions.

In an effort to develop a quantitative relationship between base pairing strength and functional stability, we use an intramolecularly folding DNA triplex (*31*, *32*) to model the folding of RNAs that have function by virtue of their tertiary folding. A triplex was chosen because, in contrast to the larger RNAs (*11*, *33*), it is a relatively simple three-state sequential folder. In addition, tertiary structure can be strengthened by lowering pH, which drives formation of C^+•GC base triples (*34*−*38*). Last, we designed our triplex with a flanking tunable region that contains base pairs completely separate from tertiary interactions. This was done to investigate the extent to which secondary structural elements *not involved in tertiary interactions* affect the thermostability of nearby tertiary interactions.

We show that the functional stability of a DNA triplex at high temperature is influenced by secondary structure stability separate from the site of tertiary interactions, but only when folding is cooperative (at pH 5.5). Under noncooperative conditions (at pH 7.0), functional stability is independent of secondary structure stability. This linkage between cooperativity and functional stability is similar to that determined in large catalytic RNAs, which have more complex folding pathways (*8*, *39*). We emphasize the distinction between *tertiary structure stability* and *thermostability* since tertiary structure stability, at least in our model system, is independent of secondary structure stability, while thermostability is not. Because the stability of RNA secondary structure follows relatively straightforward rules and can be drastically changed by one or two mutations (*13*), these observations suggest a simple mechanism for thermophilic adaptation of functional RNAs.

MATERIALS AND METHODS

DNA Design. Following are the DNA sequences used in this study. As an example of the notation, the designation

GGGG triplex: 5′-AGAGAGAGGGG*TTTTT*CCCCTCTCTCT*TTTTT*-TCTCTCT
AGGG triplex: 5′-AGAGAGAAGGG*TTTTT*CCCTTCTCTCT*TTTTT*-TCTCTCT
AAGG triplex: 5′-AGAGAGAAAGG*TTTTT*CCTTTCTCTCT*TTTTT*-TCTCTCT
AAAG triplex: 5′-AGAGAGAAAAG*TTTTT*CTTTTCTCTCT*TTTTT*-TCTCTCT
AAAA triplex: 5′-AGAGAGAAAAA*TTTTT*TTTTTCTCTCT*TTTTT*-TCTCTCT
G***G***GG triplex: 5′-AGAGAGAG***G***GG*TTTTT*CC***T***CTCTCTCT*TTTTT*-TCTCTCT
GGGG triplex: 5′-AGAGAGA***GG***GG*TTTTT*CC***TT***TCTCTCT*TTTTT*-TCTCTCT
GGGG duplex: 5′-AGAGAGAGGGG*TTTTT*CCCCTCTCTCT
AAAA duplex: 5′-AGAGAGAAAAA*TTTTT*TTTTTCTCTCT

"GGGG" means that there are four GC pairs in the tunable region, which is underlined along with its Watson−Crick complement. The duplex sequences lack the final twelve nucleotides. Loops of five Ts are italicized; these were chosen to provide flexibility for the triplex to fold, while avoiding changes in protonation state at lower pH (*40*). ***G*** and ***T*** in bold and italic font signify a GT wobble pair. The C^+•GC and T•AT triples alternate to prevent fraying of triples at the helical termini (*38*) and to prevent electrostatic repulsions that would arise from adjacent C^+•GC triples.

DNA Preparation. DNA oligonucleotides were obtained from Integrated DNA Technologies (Coralville, IA). Samples were desalted by dialysis against deionized water using a microdialysis system (Gibco-BRL Life Technologies). Buffers consisted of 5 mM dibasic sodium phosphate; pH was adjusted with HCl. Electrospray ionization LC mass spectrometry data were acquired to confirm oligonucleotide identity and purity (see Supporting Information).

[1] Abbreviations: T_M, melting temperature; TMT, tertiary structure melting temperature.

Table 1: Thermodynamic Parameters for Triplex Formation at pH 7.0[a]

sequence	ΔG_{23} (kcal/mol)	$\Delta\Delta G_{23}$ (kcal/mol)	T_{M23} (TMT) (°C)	ΔT_{M23} (°C)	ΔG_{12} (kcal/mol)	$\Delta\Delta G_{12}$ (kcal/mol)	T_{M12} (°C)	ΔT_{M12} (°C)
Watson−Crick								
GGGG	5.43 ± 0.14	−	21.8 ± 0.5	−	−1.56 ± 0.09	−	56.5 ± 0.3	−
AGGG	5.31 ± 0.16	−0.11 ± 0.21	22.1 ± 0.2	0.3 ± 0.5	−0.60 ± 0.06	0.95 ± 0.11	52.5 ± 0.2	−4.0 ± 0.4
AAGG	5.32 ± 0.10	−0.10 ± 0.17	22.0 ± 0.4	0.3 ± 0.6	0.22 ± 0.05	1.78 ± 0.10	49.1 ± 0.2	−7.4 ± 0.4
AAAG	5.43 ± 0.13	0.01 ± 0.19	21.6 ± 0.5	−0.2 ± 0.7	1.17 ± 0.08	2.73 ± 0.12	45.1 ± 0.4	−11.4 ± 0.5
AAAA	5.64 ± 0.07	0.22 ± 0.16	21.1 ± 0.3	−0.7 ± 0.6	1.94 ± 0.11	3.49 ± 0.14	42.1 ± 0.3	−14.4 ± 0.4
non-Watson−Crick[b]								
G***G***GG	5.65 ± 0.19	0.23 ± 0.24	21.0 ± 0.6	−0.7 ± 0.8	0.58 ± 0.09	2.13 ± 0.13	47.2 ± 0.5	−9.3 ± 0.6
GGGG	*not a clean transition*					*not a clean transition*		
duplexes[c]								
GGGG					−2.03 ± 0.11	−0.48 ± 0.14	59.0 ± 0.3	2.5 ± 0.4
AAAA[d]					1.11 ± 0.05	−0.83 ± 0.12	45.0 ± 0.3	2.9 ± 0.4

[a] All melts were performed in 10 mM Na^+ as described in Materials and Methods. The provided ΔG values are at 50 °C since this is closer to T_{M12} and more relevant to the temperatures at which thermophiles live. The TMT is the temperature at which tertiary structure is lost, and is equivalent to T_{M23} under noncooperative conditions of pH 7.0. [b] Non-Watson−Crick refers to GT wobble pairs at the underlined positions. [c] "Duplex" refers to hairpin oligonucleotides that mimic the duplex intermediate. [d] The reference state for duplex AAAA is triplex AAAA.

Determination of Thermodynamic Parameters by UV Melting. UV melting experiments were performed on a Gilford Response II spectrophotometer with a data point acquired every 0.5 °C and a heating rate of ~0.6 °C/min at 260 nm. Melts from 95 to 5 °C and 5 to 95 °C provided data consistent with reversibility of folding transitions (*41*). Melts were normalized by dividing absorbances collected as a function of temperature by the high-temperature absorbance value. Monophasic melt data were fit to a two-state model using sloping baselines and analyzed using a Marquadt algorithm for nonlinear curve fitting in KaleidaGraph v.3.5 (Synergy software). Thermodynamic parameters are the average from at least three independently prepared samples. For the three-state melt data, the two transitions were fit separately using the two-state model. Representative melts were also fit directly by a three-state model (*41*) and gave similar parameters (not shown). Derivative plots were of normalized data and were smoothed using an 11 point window. Noncooperative data (pH 7.0) are presented in Tables 1 and S1, while cooperative data (pH 5.5) are presented in Tables 2 and S2; Tables S1 and S2 are published as Supporting Information.

Assignment of Thermodynamic States by Circular Dichroism. Circular dichroism spectra were collected on a JASCO 810 spectropolarimeter from 320 to 200 nm with a step of 1.0 nm and a 2 s averaging time. Buffer spectra were subtracted, and the signal was normalized to molar circular dichroic absorption ($\Delta\epsilon$) (*42*). Spectra were averaged and smoothed over a five-point window.

RESULTS AND DISCUSSION

Design of the Intramolecularly Folding DNA Triplexes. Triplexes are typically composed of a homopurine−homopyrimidine Watson−Crick helix and a third strand. The third strand inserts into the major groove of the helix and, when composed of pyrimidines, runs parallel to the purine strand and interacts with it via Hoogsteen base pairing to form T•AT or C^+•GC base triples (*43*). Triplexes have been demonstrated to form *in vivo* (*31*) and are being actively pursued in therapeutic applications (*44*); they can be composed of multiple strands or can form intramolecularly (*32, 43*). Here, we used triplexes as the experimental basis to investigate the linkage between secondary structure stability and functional stability.

Table 2: Thermodynamic Parameters for Triplex Formation at pH 5.5[a]

sequence	ΔG_{obs}[b] (kcal/mol)	$\Delta\Delta G_{obs}$ (kcal/mol)	T_{Mobs} (~TMT) (°C)	ΔT_{Mobs} (°C)
Watson−Crick				
GGGG	−1.44 ± 0.06	−	56.7 ± 0.3	−
AGGG	−1.20 ± 0.09	0.24 ± 0.11	55.0 ± 0.5	−1.7 ± 0.5
AAGG	−0.80 ± 0.08	0.64 ± 0.10	53.0 ± 0.3	−3.6 ± 0.4
AAAG	−0.19 ± 0.09	1.25 ± 0.11	50.7 ± 0.3	−6.0 ± 0.5
AAAA	0.26 ± 0.08	1.70 ± 0.10	49.1 ± 0.3	−7.6 ± 0.4
non-Watson−Crick[c]				
GGGG	−0.11 ± 0.11	1.32 ± 0.13	50.4 ± 0.4	−6.2 ± 0.5
GGGG	2.03 ± 0.05	3.46 ± 0.08	42.6 ± 0.3	−14.0 ± 0.4
duplexes[d]				
GGGG	−1.50 ± 0.01	−0.07 ± 0.07	59.0 ± 0.1	2.4 ± 0.3
AAAA[e]	0.78 ± 0.04	0.52 ± 0.09	46.5 ± 0.3	−2.5 ± 0.4

[a] All melts were performed in 10 mM Na^+ as described in Materials and Methods. [b] The provided ΔG values are observed values ("obs") determined from fits to a two-state model, extrapolated to 50 °C since this is closer to the observed T_M. Because the observed values are for loss of tertiary structure, they are used as an operational definition of ΔG_f in the text and in Figure 4. ΔG_{obs} and T_{Mobs} values are approximately equal to ΔG_{13} and T_{M13} under the cooperative conditions of pH 5.5, as described in the text. [c] Non-Watson−Crick refers to GT wobble pairs at the underlined positions. [d] "Duplex" refers to hairpin oligonucleotides that mimic the duplex intermediate. For duplexes, the values provided are for the 1° to 2° structure transition. [e] The reference state for duplex AAAA is triplex AAAA.

We chose to model the hierarchical folding of RNA through the simpler sequential folding of intramolecular triplexes. In addition to the base triples and loops typically present in intramolecular triplexes (*32, 34−38*), we included a four-base-pair cassette, or "tunable region", adjacent to the triplex (Figure 1, green). The GC-content of the tunable region was altered to test experimentally the effect of secondary structure stability on functional stability; the base triples and loops were kept constant in all of the triplex variants studied. Formation of essentially equivalent native structures by the triplexes is supported by native gel electrophoresis experiments (Figure S1, published as Supporting Information). As shown below, unfolding of each triplex is consistent with two transitions: one between primary (random coil) and secondary structure, described with an equilibrium constant for folding of K_{12}, and another between secondary and tertiary structure, with an equilibrium

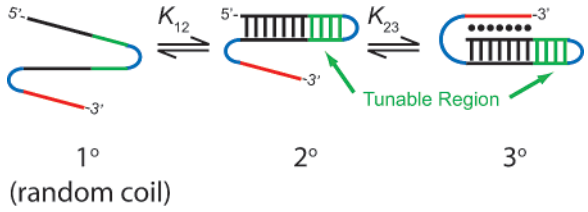

FIGURE 1: General structure of intramolecular DNA triplexes and their sequential folding pathway. Each triplex comprises a Watson−Crick base-pairing region (black) that forms seven base triples with the 3′-terminal portion of the sequence (red), a four-base-pair tunable region that does not participate in triplex formation (green), and two T5 loops (blue). Loops and triplex strand sequences are identical for each variant. Folding initiates with formation of secondary structure (2°) from random coil (1°) with an equilibrium constant of K_{12}, and is followed by formation of tertiary structure (3°) with an equilibrium constant of K_{23}.

constant of K_{23} (Figure 1). For certain triplexes, melting of duplex-forming sequences that lack the triplex-forming nucleotides was analyzed to directly obtain K_{12}.

Secondary Structure Stability Has No Effect on the TMT of a Noncooperative Folding System. Thermal denaturation of the triplex with GGGG (i.e., four GC base pairs) as the tunable region was performed at pH values ranging from 5.5 to 7.0. These experiments were done under low salt conditions (10 mM Na^+) for which triplex folding tends to be more cooperative (*38*). First derivative plots are shown in Figure 2, and the raw data are presented in Figure S2, published as Supporting Information. At pH 7.0, two well-separated melting transitions were present (Figure 2A). As pH is lowered, the melting transitions coalesced, until at pH 5.5 only one sharp unfolding transition was present. This is similar to behavior reported for intramolecular triplexes without a tunable region (*38*) and is due to strengthening of the C^+•GC base triples with lowering of pH (*38*, *45*). More acidic pH values were avoided because, although they further stabilize the folded state free energy, they more strongly stabilize the random coil state on account of its greater number of H^+-binding sites, leading to net acid-destabilization of the triplex (*45*). The observations show that pH can be used to adjust the folding cooperativity from none at higher pH, to high at lower pH, where cooperativity is defined as "the depletion of intermediate states" (*46*), herein the duplex state (Figure 1). The hyperchromicity is identical between the pH 7.0 and pH 5.5 melts (Figure S2A) despite absence of a well-populated duplex intermediate in the latter; this observation is consistent with equivalence of the initial states under both noncooperative and cooperative conditions, as well as final states.

To examine the interplay of secondary and tertiary structure, the strength of base pairing in the tunable region was modulated. A series of oligonucleotides was prepared in which the loop-distal GC base pairs were incrementally replaced with ATs, until an AAAA tunable region was present (see legend in Figure 2B). The melting profiles of these oligonucleotides were first examined under noncooperative folding conditions of pH 7.0.

As seen in Figures 2B and S2B, the higher-temperature transition was very sensitive to the base-pairing content of the tunable region. The higher-temperature T_M for the GGGG triplex was 56.5 °C, while the higher T_M for AAAA was only 42.1 °C (Table 1). The observed sequence dependence of this T_M is consistent with unfolding of secondary structure,

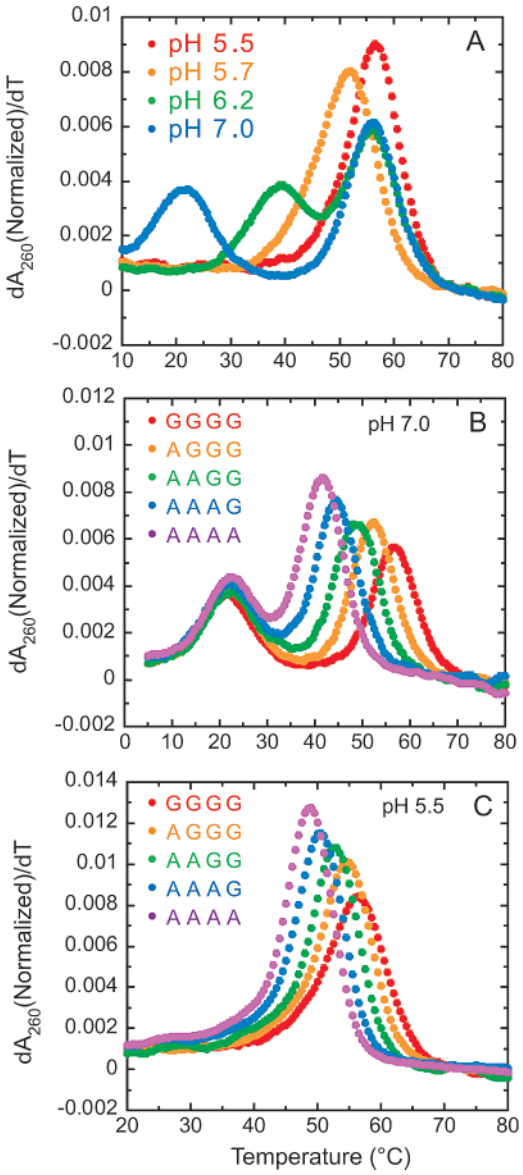

FIGURE 2: Comparison of first-derivative absorbance curves of triplex melts. (A) Curves of pH-dependent melts of triplex GGGG. At higher pH values (6.2, 7.0), two transitions are visible. The lower-temperature transition corresponds to the unfolding of the triplex, and the higher-temperature transition to unfolding of secondary structure. At lower pH values (5.5, 5.7) only one transition is observed. (B) Curves at pH 7.0 of triplexes with varied Watson−Crick base pairing in the tunable region. For each triplex there are two transitions, the second of which has a T_M value that depends on the sequence of the tunable region. (C) Curves at pH 5.5 of the same triplexes. For each triplex there is only one transition and its T_M value is dependent on the sequence of the tunable region.

as confirmed by two means. First, melting studies were performed on duplexes with the same sequence as the triplexes, but without the 3′-terminal loop and triplex-forming pyrimidines. The T_Ms for the GGGG and AAAA duplexes were 59.0 and 45.0 °C, respectively, similar to those determined for the higher T_M in triplex unfolding (Table 1 and Figure S3 [published as Supporting Information]). Second, we measured circular dichroism (CD) spectra on triplexes and duplexes at various temperatures, and the spectra were consistent with these assignments (see below). We thus assign this higher-temperature transition as T_{M12} for unfolding of secondary to primary structure.

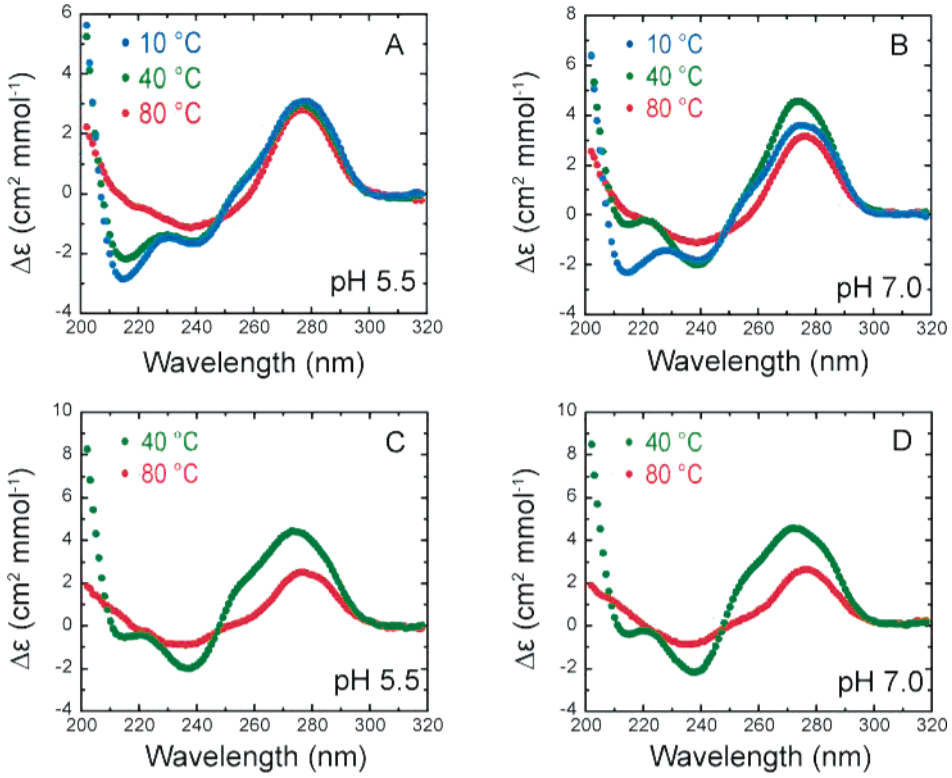

FIGURE 3: CD spectra at different temperatures of triplex GGGG and duplex GGGG. Triplex GGGG is shown at 10, 40, and 80 °C in (A) and (B) at pH 5.5 and 7.0, respectively. Duplex GGGG is shown at 40 and 80 °C in (C) and (D) at pH 5.5 and 7.0, respectively. See text for interpretation.

In contrast to T_{M12}, the lower-temperature T_M at pH 7.0 was insensitive to the base-pairing content of the tunable region. Within experimental error, the GGGG triplex had the same T_M as AAAA, 21.8 and 21.1 °C respectively; likewise, the sequences with intermediate AT content (or 1 GT wobble) had the same T_M (Table 1 and Figure S4, published as Supporting Information). In addition, the free energy change (ΔG) for this transition was identical for this series of oligonucleotides (Table 1). Since the higher-temperature T_M was assigned to secondary structure unfolding, this lower-temperature T_M should be for unfolding of tertiary structure into secondary structure. This was confirmed by CD measurements (see below). We therefore assign this low-temperature transition as T_{M23}. Overall, under noncooperative (pH 7.0) folding conditions, the TMT (T_{M23}) is independent of the strength of base pairing, and functional stability ΔG_f ($\approx\Delta G_{23}$ under noncooperative conditions; see Supporting Information) is unaffected by secondary structure stability.

Secondary Structure Stability Increases the TMT of a Cooperative Folding System. We also examined the melting profile of the same series of oligonucleotides under cooperative folding conditions of pH 5.5. As seen in Figures 2C and S2C, the single folding transition was sensitive to the base-pairing content of the tunable region. The GGGG triplex had a T_M of 56.7 °C, while AAAA had a T_M of only 49.1 °C (Table 2). Likewise, the folding transition was sensitive to GT wobble content of the tunable region (Table 2 and Figure S4).

The behavior of this transition at pH 5.5 is consistent with unfolding of tertiary structure directly to primary structure. As mentioned, the hyperchromicity was identical between the low and high pH melts (Figure S2A and S3A), and the CD spectra for the low and high temperature states at pH 5.5 were consistent with unfolding from tertiary structure directly to primary structure (see below). Thus, under cooperative (pH 5.5) folding conditions, the TMT ($\approx T_{M13}$) is favored by stronger base pairing, as is observed functional stability ΔG_f ($\approx\Delta G_{13}$ under cooperative conditions; see Supporting Information).

Assignment of States by Circular Dichroism. CD spectra (Figure 3) of the GGGG triplex were acquired as a function of temperature, choosing temperatures at which each of the three states would be maximally populated. Inspection of unfolding curves (Figure 2A) indicated that 10, 40, and 80 °C should primarily populate the folded, intermediate, and unfolded states at pH 7.0, respectively. In contrast, at pH 5.5 only two states should be populated: the folded state at 10 and 40 °C, and the unfolded state at 80 °C. The pH 5.5 CD spectra showed a unique signature of high and moderate negative ellipticity at ~215 and 240 nm at both 10 and 40 °C, while the pH 7.0 spectra showed this feature only at 10 °C (Figure 3A, 3B). In contrast, the 40 °C spectrum at pH 7.0 had the ellipticity ratio of these two peaks switched, consistent with population of a new state. At 80 °C, the rather featureless spectra were identical between pH 5.5 and 7.0 and distinct from any of the lower temperature spectra, consistent with population of the unfolded state. To confirm the identities of these states, CD spectra were acquired on the duplex control sequences at both pH values (Figure 3C, 3D). The spectra at 40 °C for the duplex were similar at pH 5.5 and 7.0, and similar to that for the GGGG triplex at pH 7.0 and 40 °C, confirming the assignment of this state to the duplex. No state with this signature was found for the GGGG triplex sequence at pH 5.5, consistent with cooperative folding. In addition, at 80 °C the duplex control

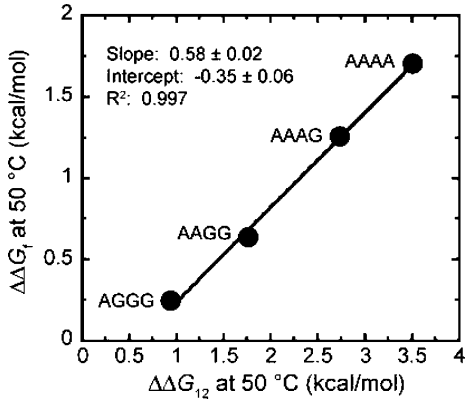

FIGURE 4: Linear free energy relationship between $\Delta\Delta G_f$ at pH 5.5 (set equal to $\Delta\Delta G_{obs}$ from Table 2) and $\Delta\Delta G_{12}$ at pH 7.0 (from Table 1) at 50 °C for triplexes with Watson−Crick base pairs in the tunable region. As described in Table 2, under these conditions $\Delta G_f \approx \Delta G_{13}$.

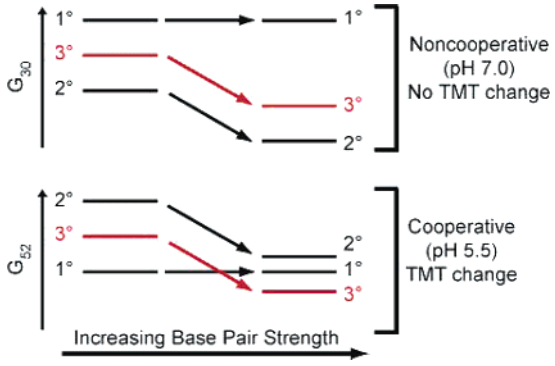

FIGURE 5: Isothermal free energy diagrams for triplex formation. The left-hand side shows energies of the states of Figure 1 at temperatures just above the TMT for the AAAA triplex. The right-hand side shows effects of strengthening secondary structure by changing the tunable region to GGGG. Strengthening base pairing in the tunable region affects the energy levels of the secondary and tertiary structure states equally and in a largely pH-independent fashion. The upper portion of the figure is at noncooperative (pH 7.0) conditions and a temperature of 30 °C, while the lower portion is at cooperative (pH 5.5) conditions and a temperature of 52 °C (see Figure 6). Strengthening base pairing leads to no change in the TMT at pH 7.0 but to an increase in TMT at pH 5.5.

sequences gave the same spectra as the triplex sequences, consistent with all sequences being in the fully unfolded random coil state when well above their higher T_M. In summary, the CD spectra fully support the assignment of the three states in the pH 7.0 unfolding as triplex, duplex, and unfolded, and the two states in the pH 5.5 unfolding as triplex and unfolded.

Model for Functional Stability Increasing with Secondary Structure Stability. The experimental data on the triplex oligonucleotides are consistent with the secondary structure adjacent to the tertiary structure influencing functional stability only under cooperative folding conditions. The contribution of secondary structure stability to functional stability under cooperative conditions is quantitatively assessed in Figure 4. This figure shows a plot of $\Delta\Delta G_f$ under cooperative folding conditions ($\Delta\Delta G_{obs}$ pH 5.5) versus $\Delta\Delta G_{12}$ (secondary structure stability at pH 7.0), both evaluated at 50 °C, which is near their respective T_Ms and relevant to the temperatures at which moderate thermophiles live. (Recall that $\Delta G_f \approx \Delta G_{13}$ under cooperative conditions, and ΔG_{obs} at pH 5.5 is an operational definition of ΔG_f; see Figure 5 and Table 2.) The four points are for the sequences with Watson−Crick base pairing in the tunable region, with ΔG values relative to the GGGG triplex. Observed stability and secondary structure stability show a linear free energy relationship, with a slope of ~0.6.[2] This relationship illustrates that, under cooperative folding conditions, secondary structure free energy is directly transferable to functional free energy. Several reasons may explain why only 60% of the secondary structure energy is transferred into functional stability. One possibility is the absence of complete cooperativity at pH 5.5: the duplex for GGGG has a population of ~25% at pH 5.5 (Figure S5E, published as Supporting Information), and the duplex for AAAA has a population of ~8% at pH 5.5 (Figure S5G). Other possibilities include slight effects of the triples on base-pairing geometry or small effects of pH on base-pairing stability. As shown in Table 2, there is also a monotonic increase in TMT with strength of secondary structure in the tunable region.

To gain further insight into the mechanism for TMT increase with base pairing, we present free energy schemes for triplex unfolding at both high and low pH (Figure 5). The left-hand side of Figure 5 depicts the ordering of free energies of the three states of Figure 1 at temperatures just above the TMTs. At high pH, this corresponds to the tertiary structure state lying above the secondary but below the primary structure state (random coil), while at low pH, this corresponds to the tertiary structure state lying above the primary but below the secondary structure state. Increasing base pairing strength in the tunable region (i.e., going to the right-hand side of Figure 5) leads to equivalent lowering of secondary and tertiary states (at both pHs) because both states contain equivalent base pairing. Under noncooperative folding conditions of pH 7.0, the ordering of the three states is unchanged, consistent with the observed inability of base-pairing strength to affect the TMT (Table 1, column 4). However, under cooperative folding conditions of pH 5.5, the free energy of the tertiary structure state crosses the free energy of the primary structure state, leading to a reordering of the free energies of these three states and resulting in tertiary structure now being the most stable state for this new sequence at this temperature. This reordering of the three states explains the observed ability of increased base-pairing strength to translate into an increase in thermostability under cooperative folding conditions (Table 2, column 4).

To help understand the temperature dependence of free energy, simulations were performed for both cooperative and noncooperative folding conditions for the two limiting triplex sequences, GGGG and AAAA. These simulations use the thermodynamic parameters measured for triplexes and duplexes (see the tables), with details of the simulation procedure and equations described fully in Supporting Information. Briefly, we transformed the Sosnick and Pan definition of functional stability (*8*) into a mathematical

[2] The contribution of secondary structure stability to functional stability was also assessed at a constant pH of 5.5 by melting duplexes representing each of the five non-GT-containing triplexes at this pH. The free energy relationship was linear with an R^2 value of 0.993 and a slope of 0.86 (data not shown). We opt to discuss the pH 7.0 duplex melts herein because their energies reflect the full triplex sequence and because they were conducted at near-physiological pH. Nevertheless, the slope for the pH 7.0 case should be taken as a conservative estimate to the contribution of secondary structure stability to functional stability.

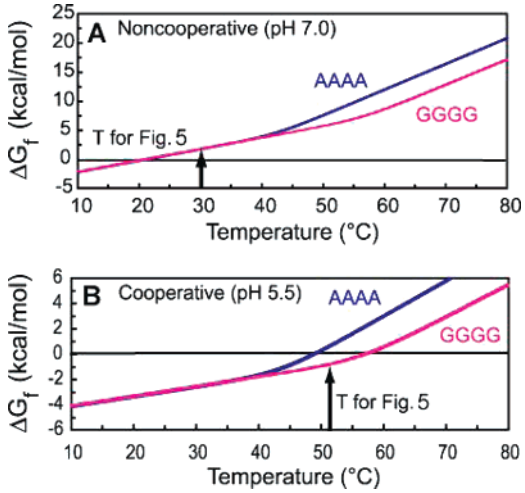

FIGURE 6: Simulations of functional free energy change ΔG_f for triplexes GGGG (magenta) and AAAA (blue). The plots of ΔG_f versus temperature use parameters from the tables. The observed TMT is the temperature at which a curve crosses the $\Delta G_f = 0$ line. Marked are the temperatures at which the corresponding free energy diagrams were drawn in Figure 5. (A) Plots for triplexes GGGG and AAAA under noncooperative conditions (pH 7.0). (B) Plots for triplexes GGGG and AAAA under cooperative conditions (pH 5.5).

equation. We define a functional equilibrium constant as the concentration of the triplex state relative to the sum of the concentrations of all other states, which allows the identity of the penultimately stable state (i.e., reference state) to change with temperature. The functional thermodynamic parameters were then calculated by applying standard thermodynamic relationships. This approach leads to a piecewise linear free energy−temperature profile.

Simulations with the pH 7.0 data illustrate the dependence of ΔG_f on temperature for the GGGG and AAAA triplexes under noncooperative folding conditions (Figure 6A). A species plot shows that the duplex intermediate populates to ~99%, consistent with complete absence of cooperativity under these conditions (Figure S5). We note that, at $\Delta G_f = 0$, the temperature is the TMT because half of the molecules are in the functional state (i.e., have tertiary structure). The simulations show that the divergence in ΔG_f between the GGGG and AAAA triplexes occurs at temperatures well above the TMT, and so "functional" tertiary structure is lost at the same (low) temperature for both triplexes (Figure 6A). For these noncooperative conditions, $\Delta G_f \approx \Delta G_{23}$ near the TMT.

The calculated dependence of ΔG_f on temperature for the GGGG and AAAA triplexes under cooperative (pH 5.5) folding conditions is depicted in Figure 6B. At low temperatures, the ΔG_f values for the two sequences coincide because secondary structure is stable at these temperatures and is the penultimately stable state; thus, in general, sequences with different base pairing strength are predicted to have the same functional stability at lower temperatures. This offers an explanation as to why base-pairing changes do not have an appreciable effect on tertiary unfolding when certain RNAs are assayed by native gels at lower temperatures (*26*) (S.K.S. and P.C.B., unpublished data). However, when the T_M for secondary structure without accompanying tertiary structure is exceeded, the temperature dependence of ΔG_f becomes much steeper; this is because the penultimately stable folding state has changed to primary structure. This effect can also be seen in the temperature dependence of ΔH_f (Figure S5C). Because GGGG has more stable base pairing than AAAA, its "flex point" for switching into this steeper regime occurs at a higher temperature. As a consequence, the temperature at which the $\Delta G_f = 0$ line is crossed (TMT) is higher. In summary, the melting temperature of the underlying secondary structure acts as the "trigger" to enter into the cooperative unfolding phase. Therefore, in the context of equally stable tertiary structure, secondary structure stability controls the TMT. For these cooperative conditions, $\Delta G_f \approx \Delta G_{13}$ near the TMT.

Strikingly, in these simulations exactly the same tertiary structure stability was used for both GGGG and AAAA triplexes, as dictated by experimental determinations of ΔG_{23} at pH 7.0. *Thus, the observed differences in thermostability between these sequences is unrelated to the strength of tertiary structure.* The necessity for high cooperativity to attain a higher TMT is in line with observations on RNase P RNAs, wherein RNAs were found to be more stable when folding cooperativity was enhanced (*8*, *39*). Despite this similarity, folding is appreciably more complex in those other systems, and any linkage of folding cooperativity to secondary structure stability is unclear at present.

Implications for Thermophilic Adaptation in Functional Nucleic Acids. We have presented experimental data, as well as a free energy scheme and simulations, that lead to a model in which base pairing separate from tertiary interactions allows a functional nucleic acid to retain its function at higher temperature. Coupled equilibria maintain the three-state hierarchical folding (Figure 1) in which secondary structure precedes tertiary structure formation thermodynamically and kinetically, a framework that is widely accepted for RNA folding and indeed physically demanded by the system. Hierarchical folding has been argued to underlie the folding of simple and complex proteins (*47*, *48*). To explain our data, we do not need to invoke a more complicated folding pathway such as four-state folding in which residual secondary structure forms after tertiary structure, four-state folding in which misfolded secondary structure is resolved after tertiary structure formation, or a branched pathway.

Our impetus for this study was the paradoxical observation that functional RNAs from thermophiles tend to have more stable secondary structures than their mesophilic counterparts (*22*−*25*), yet tertiary structure stability is not related to the strength of preformed base pairs. The definition of functional stability as the stability of the tertiary state relative to the penultimately stable state (*8*) provides an escape from this paradox. By allowing the identity of the penultimately stable state to change with temperature, a non-two-state folding system can gain contributions from base pairing when folding becomes cooperative. Indeed, our data show that the TMT of a functional nucleic acid can increase without any change in the underlying stability of tertiary structure. This model has implications for the evolution of RNA.

Sosnick and Pan pointed out two limiting models by which an organism can adapt its RNAs to higher temperatures: it could strengthen tertiary interactions, or it could shift the reference state to have less structure (*49*). Our data speak to the second model, and we note that the less structured state could be one without appreciable base pairing, which enables the simple adaptive mechanism of increasing the TMT by

strengthening base pairing. A key feature of this mechanism is that the altered base pairs do not even have to participate in tertiary interactions (Figure 1) as long as they are physically connected to the base pairs that do participate in tertiary interactions (e.g., part of the same helix). As such, an RNA could in principle adapt to higher temperatures simply by acquiring point mutations that alter the secondary structure, such as changing of GU wobble pairs to GC or AU pairs, or deletion of helical bulges, both of which Juneau and Cech found in sequence analysis of *in vitro* evolution experiments (*26*). Because tertiary structure-forming nucleotides do not have to change in this mechanism, function should be retained. Thus, this mechanism provides a simple and convenient means of thermophilic adaptation.

In addition, this mechanism provides an energetically powerful means of adaptation. For instance, a GU to GC change can be worth as much as −1.5 kcal/mol in folding free energy; deletion of a bulged nucleotide contributes ∼−3.9 kcal/mol; and insertion of a base opposite a bulge can contribute up to −7.3 kcal/mol (*50*). Given the slope of ∼0.6 in the linear free energy relationship (Figure 4), these point mutations potentially contribute between ∼−1 and −4 kcal/mol to functional folding stability, where the latter value is worth approximately a factor of 10^3 in the equilibrium constant at 37 °C. Thus, this model offers a quantitative explanation for why the GC content of stems in ribosomal and transfer RNAs is high for thermophiles while the overall genomic GC content is not (*23*), as well as for why some thermophilic RNAs contain relatively few secondary structure defects (*22*).

The thermodynamic driving force for tertiary interactions in RNA, while not extensively studied, is often entropic (*51*−*53*), suggesting that tertiary interactions may persist at the high temperatures at which thermophiles live. The association of Mg^{2+} with ATP is also known to be entropically driven (*54*), implying that metal−RNA interactions, typical of tertiary structure formation, could be endothermic. Nevertheless, in some cases, tertiary structures may be melted at thermophilic temperatures, and so tertiary structure may have to be strengthened for thermophilic adaptation (*49*, *55*). In addition, cellular factors such as proteins and crowding agents may contribute to the stability of RNA at thermophilic conditions.

Despite the above caveats, the preponderance of stable secondary structures in functional RNAs from thermophiles (*23*) along with our quantitative findings relating secondary structure stability and functional stability suggest that strengthening of base pairing is an important mechanism for achieving thermostability. Because base pairing affects thermostability only when folding is cooperative and base pairing is GC-rich in functional thermophilic RNAs, the folding transition that leads to function for many thermophilic RNAs may involve the formation of at least some secondary structure. This seems reasonable given the high temperatures at which these organisms live.

ACKNOWLEDGMENT

We thank Doug Turner and Tina Henkin for stimulating discussions, Becky Toroney for discussions on triplex design, and Nate Siegfried and Josh Sokoloski for comments on the manuscript. We also thank Ellen Moody for performing early versions of the simulations.

SUPPORTING INFORMATION AVAILABLE

Native polyacrylamide gel experiment, representative melting curves for all sequences, representative derivative plots, mass spectrometry analysis, and procedure for simulations. This material is available free of charge via the Internet at http://pubs.acs.org.

REFERENCES

1. Ban, N., Nissen, P., Hansen, J., Moore, P. B., and Steitz, T. A. (2000) The complete atomic structure of the large ribosomal subunit at 2.4 Å resolution, *Science 289*, 905−920.
2. Doudna, J. A., and Cech, T. R. (2002) The chemical repertoire of natural ribozymes, *Nature 418*, 222−228.
3. Fedor, M. J., and Williamson, J. R. (2005) The catalytic diversity of RNAs, *Nat. Rev. Mol. Cell Biol. 6*, 399−412.
4. Hougland, J. L., Piccirilli, J. A., Forconi, M., Lee, J., and Herschlag, D. (2006) How the group I intron works: A case study of RNA structure and function, in *RNA World*, 3rd ed. (Gesteland, R. F., Cech, T. R., and Atkins, J. F., Eds.) pp 133−205, Cold Spring Harbor Press, Cold Spring Harbor, New York.
5. Bevilacqua, P. C., and Yajima, R. (2006) Nucleobase catalysis in ribozyme mechanism, *Curr. Opin. Chem. Biol. 10*, 455−464.
6. Tucker, B. J., and Breaker, R. R. (2005) Riboswitches as versatile gene control elements, *Curr. Opin. Struct. Biol. 15*, 342−348.
7. Herschlag, D. (1995) RNA chaperones and the RNA folding problem, *J. Biol. Chem. 270*, 20871−20874.
8. Fang, X. W., Golden, B. L., Littrell, K., Shelton, V., Thiyagarajan, P., Pan, T., and Sosnick, T. R. (2001) The thermodynamic origin of the stability of a thermophilic ribozyme, *Proc. Natl. Acad. Sci. U.S.A. 98*, 4355−4360.
9. Brown, T. S., Chadalavada, D. M., and Bevilacqua, P. C. (2004) Design of a highly reactive HDV ribozyme sequence uncovers facilitation of RNA folding by alternative pairings and physiological ionic strength, *J. Mol. Biol. 341*, 695−712.
10. Woodson, S. A. (2005) Metal ions and RNA folding: a highly charged topic with a dynamic future, *Curr. Opin. Chem. Biol. 9*, 104−109.
11. Talkington, M. W., Siuzdak, G., and Williamson, J. R. (2005) An assembly landscape for the 30S ribosomal subunit, *Nature 438*, 628−632.
12. Holbrook, S. R. (2005) RNA structure: the long and the short of it, *Curr. Opin. Struct. Biol. 15*, 302−308.
13. Mathews, D. H., and Turner, D. H. (2006) Prediction of RNA secondary structure by free energy minimization, *Curr. Opin. Struct. Biol. 16*, 270−268.
14. Brion, P., and Westhof, E. (1997) Hierarchy and dynamics of RNA folding, *Annu Rev. Biophys. Biomol. Struct. 26*, 113−137.
15. Tinoco, I., Jr., and Bustamante, C. (1999) How RNA folds, *J. Mol. Biol. 293*, 271−281.
16. Crothers, D. M., Cole, P. E., Hilbers, C. W., and Shulman, R. G. (1974) The molecular mechanism of thermal unfolding of *Escherichia coli* formylmethionine transfer RNA, *J. Mol. Biol. 87*, 63−88.
17. Stein, A., and Crothers, D. M. (1976) Conformational changes of transfer RNA. The role of magnesium(II), *Biochemistry 15*, 160−168.
18. Laing, L. G., Gluick, T. C., and Draper, D. E. (1994) Stabilization of RNA structure by Mg ions. Specific and non-specific effects, *J. Mol. Biol. 237*, 577−587.
19. Gluick, T. C., and Draper, D. E. (1994) Thermodynamics of folding a pseudoknotted mRNA fragment, *J. Mol. Biol. 241*, 246−262.
20. Nixon, P. L., and Giedroc, D. P. (1998) Equilibrium unfolding (folding) pathway of a model H-type pseudoknotted RNA: the role of magnesium ions in stability, *Biochemistry 37*, 16116−16129.
21. Jaenicke, R., and Bohm, G. (1998) The stability of proteins in extreme environments, *Curr. Opin. Struct. Biol. 8*, 738−748.
22. Brown, J. W., Haas, E. S., and Pace, N. R. (1993) Characterization of ribonuclease P RNAs from thermophilic bacteria, *Nucleic Acids Res. 21*, 671−679.
23. Galtier, N., and Lobry, J. R. (1997) Relationships between genomic G+C content, RNA secondary structures, and optimal growth temperature in prokaryotes, *J. Mol. Evol. 44*, 632−636.

24. Wang, H. C., and Hickey, D. A. (2002) Evidence for strong selective constraint acting on the nucleotide composition of 16S ribosomal RNA genes, *Nucleic Acids Res. 30*, 2501−2507.
25. Lu, Z. J., Turner, D. H., and Mathews, D. H. (2006) A set of nearest neighbor parameters for predicting the enthalpy change of RNA secondary structure formation, *Nucleic Acids Res. 34*, 4912−4924.
26. Juneau, K., and Cech, T. R. (1999) In vitro selection of RNAs with increased tertiary structure stability, *RNA 5*, 1119−1129.
27. Laing, L. G., and Draper, D. E. (1994) Thermodynamics of RNA folding in a conserved ribosomal RNA domain, *J. Mol. Biol. 237*, 560−576.
28. Draper, D. E., Bukhman, Y. V., and Gluick, T. C. (2000) Thermal Methods for the Analysis of RNA Folding Pathways, in *Current Protocols in Nucleic Acid Chemistry* (Beaucage, S. L., Bergstrom, D. E., Glick, G. D., and Jones, R. A., Eds.) pp 11.13.1−11.13.13, John Wiley & Sons, Inc., New York.
29. Schaak, J. E., Babitzke, P., and Bevilacqua, P. C. (2003) Phylogenetic conservation of RNA secondary and tertiary structure in the *trpEDCFBA* operon leader transcript in *Bacillus*, *RNA 9*, 1502−1515.
30. Schaak, J. E., Yakhnin, H., Bevilacqua, P. C., and Babitzke, P. (2003) A Mg^{2+}-dependent RNA tertiary structure forms in the *Bacillus subtilis trp* operon leader transcript and appears to interfere with *trpE* translation control by inhibiting TRAP binding, *J. Mol. Biol. 332*, 555−574.
31. Mirkin, S. M., Lyamichev, V. I., Drushlyak, K. N., Dobrynin, V. N., Filippov, S. A., and Frank-Kamenetskii, M. D. (1987) DNA H form requires a homopurine-homopyrimidine mirror repeat, *Nature 330*, 495−497.
32. Sklenar, V., and Feigon, J. (1990) Formation of a stable triplex from a single DNA strand, *Nature 345*, 836−838.
33. Cole, P. E., Yang, S. K., and Crothers, D. M. (1972) Conformational changes of transfer ribonucleic acid. Equilibrium phase diagrams, *Biochemistry 11*, 4358−4368.
34. Plum, G. E., and Breslauer, K. J. (1995) Thermodynamics of an intramolecular DNA triple helix: a calorimetric and spectroscopic study of the pH and salt dependence of thermally induced structural transitions, *J. Mol. Biol. 248*, 679−695.
35. Asensio, J. L., Lane, A. N., Dhesi, J., Bergqvist, S., and Brown, T. (1998) The contribution of cytosine protonation to the stability of parallel DNA triple helices, *J. Mol. Biol. 275*, 811−822.
36. Leitner, D., Schroder, W., and Weisz, K. (2000) Influence of sequence-dependent cytosine protonation and methylation on DNA triplex stability, *Biochemistry 39*, 5886−5892.
37. Hoyne, P. R., Gacy, A. M., McMurray, C. T., and Maher, L. J., 3rd. (2000) Stabilities of intrastrand pyrimidine motif DNA and RNA triple helices, *Nucleic Acids Res. 28*, 770−775.
38. Soto, A. M., Loo, J., and Marky, L. A. (2002) Energetic contributions for the formation of TAT/TAT, TAT/CGC(+), and CGC(+)/CGC(+) base triplet stacks, *J. Am. Chem. Soc. 124*, 14355−14363.
39. Fang, X. W., Srividya, N., Golden, B. L., Sosnick, T. R., and Pan, T. (2003) Stepwise conversion of a mesophilic to a thermophilic ribozyme, *J. Mol. Biol. 330*, 177−183.
40. Saenger, W. (1984) *Principles of Nucleic Acid Structure*, Springer-Verlag, New York.
41. Nakano, S., Cerrone, A. L., and Bevilacqua, P. C. (2003) Mechanistic characterization of the HDV genomic ribozyme: classifying the catalytic and structural metal ion sites within a multichannel reaction mechanism, *Biochemistry 42*, 2982−2994.
42. Cantor, C. R., and Schimmel, P. R. (1980) in *Biophysical Chemistry, Part II: Techniques for the Study of Biological Structure and Function*, W. H. Freeman, San Francisco, CA.
43. Roberts, R. W., and Crothers, D. M. (1996) Prediction of the stability of DNA triplexes, *Proc. Natl. Acad. Sci. U.S.A. 93*, 4320−4325.
44. Rogers, F. A., Lloyd, J. A., and Glazer, P. M. (2005) Triplex-forming oligonucleotides as potential tools for modulation of gene expression, *Curr. Med. Chem. Anticancer Agents 5*, 319−326.
45. Moody, E. M., Lecomte, J. T., and Bevilacqua, P. C. (2005) Linkage between proton binding and folding in RNA: A thermodynamic framework and its experimental application for investigating pKa shifting, *RNA 11*, 157−172.
46. Dill, K. A., and Bromberg, S. (2003) *Molecular driving forces: statistical thermodynamics in chemistry and biology*, Garland Science, New York.
47. Baldwin, R. L., and Rose, G. D. (1999) Is protein folding hierarchic? II. Folding intermediates and transition states, *Trends Biochem. Sci. 24*, 77−83.
48. Baldwin, R. L., and Rose, G. D. (1999) Is protein folding hierarchic? I. Local structure and peptide folding, *Trends Biochem. Sci. 24*, 26−33.
49. Sosnick, T. R., and Pan, T. (2002) Getting hotter with RNA, *Nat. Struct. Biol. 9*, 795−796.
50. Serra, M. J., and Turner, D. H. (1995) Predicting thermodynamic properties of RNA, *Methods Enzymol. 259*, 242−261.
51. Li, Y., Bevilacqua, P. C., Mathews, D., and Turner, D. H. (1995) Thermodynamic and activation parameters for binding of a pyrene-labeled substrate by the *Tetrahymena* ribozyme: Docking is not diffusion-controlled and is driven by a favorable entropy change, *Biochemistry 34*, 14394−14399.
52. Narlikar, G. J., and Herschlag, D. (1996) Isolation of a local tertiary folding transition in the context of a globally folded RNA, *Nat. Struct. Biol. 3*, 701−710.
53. Mikulecky, P. J., Takach, J. C., and Feig, A. L. (2004) Entropy-driven folding of an RNA helical junction: an isothermal titration calorimetric analysis of the hammerhead ribozyme, *Biochemistry 43*, 5870−5881.
54. Taqui Khan, M. M., and Martell, A. E. (1966) Thermodynamic quantities associated with the interaction of adenosine triphosphate with metal ions, *J. Am. Chem. Soc. 88*, 668−671.
55. Guo, F., Gooding, A. R., and Cech, T. R. (2006) Comparison of crystal structure interactions and thermodynamics for stabilizing mutations in the *Tetrahymena* ribozyme, *RNA 12*, 387−395.

BI0620003